1 The nitrogen cost of photosynthesis

2 John R Evans and Victoria C Clarke

3 ARC Centre of Excellence for Translational Photosynthesis, Research School of Biology, Australian
4 National University, Canberra, ACT 2601, Australia

5 VC Clarke ORCID 0000-0002-1028-6749

7 Abstract

8 Global food security depends on three main cereal crops (wheat, rice and maize), achieving and
9 maintaining their high yields as well as increasing future yields. Fundamental to the production of
10 this biomass is photosynthesis. The process of photosynthesis involves a large number of proteins
11 which together account for the majority of the nitrogen in leaves. As large amounts of nitrogen are
12 removed in the harvested grain, this needs to be replaced from either synthetic fertilizer or
13 biological nitrogen fixation. Knowledge about photosynthetic properties of leaves in natural
14 ecosystems is also important, particularly when we consider the potential impacts of climate change.
15 While the relationship between nitrogen and photosynthetic capacity of a leaf differs between
16 species, leaf nitrogen content provides a useful way to incorporate photosynthesis into models of
17 ecosystems and the terrestrial biosphere. This review provides a generalised nitrogen budget for a
18 C3 leaf cell and discusses the potential for improving photosynthesis from a nitrogen perspective.

21

22 Introduction

23   Just over a century has passed since the discovery of the Haber Bosch method to reduce
24 atmospheric dinitrogen and produce ammonia which paved the way for large scale production of
25 nitrogenous fertilizer. There is a close correlation between the production of nitrogenous fertilizer
26 and the production of the three key cereals that dominate the human diet (wheat, rice and maize)
27 (http://www.fao.org/faostat). Crop production reflects photosynthesis integrated over the life of the
28 crop. The process of photosynthesis requires a system that is comprised of many proteins and which
29 accounts for the majority of nitrogen in any plant. It is this large nitrogen requirement to construct a
30 photosynthetic system that results in the need for nitrogenous fertilizer by highly productive crops.

31   The photosynthetic rate and other leaf attributes have been measured for an extensive
32 number of species. By combining two attributes, nitrogen content and the leaf dry mass, both
33 expressed per unit leaf area, it is possible to predict the photosynthetic capacity. This has proved a
34 useful way of parameterising photosynthesis over large areas of natural ecosystem that is necessary
35 for global models (Rogers *et al.*, 2017a). There are differences between species in the relationship
36 between photosynthesis and leaf nitrogen content (Kattge *et al.*, 2011). These reflect underlying
37 differences in the allocation of nitrogen between proteins, their properties, or a consequence of
38 anatomical differences. Nitrogen and photosynthesis are central to each of these interrelated topics
39 (Box 1) which are considered in this review.

40 Leaf nitrogen budget

41   It is timely to revisit the nitrogen budget of a leaf. Firstly, X-ray crystallography of protein
42 complexes reveals atomic resolution, providing accurate pigment to protein stoichiometries.
43 Secondly, a vast number of proteins and their relative abundance can now be determined using
44 mass spectrometry.

45   Dividing nitrogen between different pools can take several directions. At a cellular level, one
46 can separate soluble and membrane fractions from a cell wall pool. Alternatively, one can partition
47 nitrogen between different organelles. These two approaches rely on different methodologies and
48 generally no approach accounts for all of the nitrogen. Consequently, melding together these
49 disparate pieces of information requires adjustments to reach an average total. This average may
50 not apply to a particular leaf due to effects of age, environment and species, but it provides a useful
51 common starting point for C3 species.

52   With mass spectrometry, thousands of proteins and their relative abundance in a range of
53 organisms have been measured. The PaxDb resource (Wang *et al.*, 2015) provides estimates of
54 protein abundance derived from spectral counts across many experiments and tissue types. The
55 *Arabidopsis thaliana* database comprises 46 datasets, covering 76% of the expected proteome. More
56 than 90% of protein is accounted for by the 1000 most abundant proteins. However, protein
57 quantification by mass spectrometry has an inherent bias, over representing more abundant
58 proteins when low abundance proteins fall below the instrument detection limits. Identification of
59 proteins by mass spectrometry can also be biased due to a range of factors affecting peptide
60 detection such as peptide solubility, enzymatic digestion efficacy and differing ion efficiencies
61 (reviewed in Lundgren *et al.*, 2010).
62
63   Consequently, the PaxDb values cannot be taken at face value (Li *et al.*, 2017). For example,
64 the abundance of Rubisco large subunits outnumbers that of the small subunit by more than
65 eightfold. One would expect that the amounts of these two subunits should be similar as the mature
66 Rubisco enzyme contains 8 large and 8 small subunits. Rubisco represents about 40% of soluble
67 protein (Eckardt *et al.*, 1997), or 20% of leaf nitrogen (Evans and Seemann, 1984), which equates to
68 about 119,000 ppm for each subunit (see supplementary information). Because Rubisco is such an
69 abundant protein, this potentially introduces a significant bias unless it is corrected (Li *et al.*, 2017).
70 Further, the stoichiometry in PaxDb of proteins within and between complexes does not necessarily
71 match expectations, perhaps reflecting the fact that not all proteins are quantitatively captured
72 during the tissue preparation and subsequent measurement. However, the data available from mass
73 spectrometry allows a deeper understanding of N distribution between proteins than previous
74 techniques have afforded. Moving forward, new data independent acquisition proteomic
75 techniques, such as SWATH mass spectrometry (Law and Lim, 2013) will allow greater accuracy and
76 a much finer resolution of leaf nitrogen allocation between proteins within leaves.

77   Thylakoid N costs

78   Within the chloroplast, protein complexes in the thylakoid membranes are involved with
79 light capture, photosynthetic electron transport from water to NADP, and ATP synthesis. The relative
80 abundance of these protein complexes varies in response to growth irradiance, which also changes
81 the electron transport capacity per unit of chlorophyll. It is convenient to divide thylakoid nitrogen
82 between two pools: light capture and bioenergetics. Both photosystem II and I reaction centres
83 capture light and perform electron transport, but under unstressed conditions, neither determine
84 the electron transport capacity. Consequently, it is appropriate to place them in the pool associated
85 with light capture, together with the light harvesting chlorophyll a/b complexes (LHC). The
86 distribution of chlorophyll between these complexes can be used to estimate the nitrogen

87   associated with each, if one knows the chlorophyll to protein stoichiometry (Table 1). The majority
88   of chlorophyll is associated with the LHC (56%), each of which binds 14 chlorophylls (Liu *et al.*, 2004).
89   Photosystem I with its 4 associated LHC accounts for 30% of leaf chlorophyll in complexes that bind
90   156 chlorophylls (Caspy and Nelson, 2018; Scheller *et al.*, 2001). Photosystem II with CP26 and CP29
91   bind 63 chlorophyll (Wei *et al.*, 2016) and account for the remaining 14% of chlorophyll. Putting
92   these three fractions together results in an average nitrogen cost for light capture of 37.3 mol N (mol
93   Chl)$^{-1}$ (Table 1).

94   The second thylakoid nitrogen pool, bioenergetics, is associated with photosynthetic
95   electron transport and ATP synthesis. The relative abundance of the cytochrome b6f and ATP
96   synthase complexes covary, depending on the growth irradiance and are directly correlated with the
97   electron transport capacity (Evans, 1987; Yamori *et al.*, 2011). Consequently, cytochrome f content
98   provides a way to link photosynthetic performance to the nitrogen cost of these complexes. As
99   quantitative measures of ATP synthase were lacking when the thylakoid nitrogen budget was first
100   assembled, a ratio of 1 cyt f: 1 FNR: 1.2 ATP synthase was assumed which resulted in a nitrogen cost
101   for bioenergetics of 8.85 mol N (mmol cyt f)$^{-1}$ (Evans and Seemann, 1989). Now with the PaxDb (Li *et*
102   *al.*, 2017; Wang *et al.*, 2015), we have reassessed this assumption (see supplementary information)
103   and obtained a ratio of cyt f: FNR: ATP synthase of 1: 0.85:1.35 which leads to a revised cost for
104   bioenergetics of 10.86 mol N (mmol cyt f)$^{-1}$. The actual ratio assumed for ATP synthase makes a
105   significant impact on the total nitrogen cost of bioenergetics as it represents about 80% of this pool.

106   The nitrogen cost of thylakoids with respect to their electron transport capacity can be
107   represented graphically. In Box 2, cytochrome f content per unit chlorophyll, which is directly
108   proportional to the electron transport capacity per unit chlorophyll, varies along the x axis. The total
109   thylakoid nitrogen cost per unit chlorophyll is presented on the y axis. Symbols represent actual
110   measurements taken from spinach and pea leaves that were grown under different irradiances, as
111   well as several C4 species where mesophyll and bundle sheath cells were separately analysed (Evans,
112   1987; Evans and Seemann, 1989; Ghannoum *et al.*, 2005; Terashima and Evans, 1988). The green
113   rectangle represents the average nitrogen cost of light capture associated with LHC and the two
114   photosystem complexes (37.3 mol N (mol Chl)$^{-1}$). For simplicity, minor variation in chlorophyll
115   distribution between pigment protein complexes has been ignored here (Leong and Anderson,
116   1984). The yellow triangle represents the increasing cost of nitrogen associated with bioenergetics
117   as the electron transport capacity increases per unit chlorophyll. Two upper bounds are shown
118   depending on the nitrogen cost assumed for bioenergetics (8.85 and 10.86 mol N (mmol cyt f)$^{-1}$
119   being the original and revised estimates, respectively). On average for a leaf growing in sunlight,
120   there are about 55 mol N (mol Chl)$^{-1}$ in chloroplast thylakoid membranes.

121   Nitrogen distribution within the cell

122   To establish the relative distribution of nitrogen between the cellular organelles, it is
123   necessary to juggle different sources of information as none provide the complete picture. An
124   average distribution for mature leaves of C3 plants is: chloroplast 75%, mitochondria 5%,
125   peroxisomes 2.5%, cytosol 7.5% and cell walls 10% (Li *et al.*, 2017; Makino and Osmond, 1991;
126   Onoda *et al.*, 2017; Wang *et al.*, 2015). Alternatively, one can group the nitrogen distribution by
127   function and superimpose this onto the organellar structure (Box 3). The relative size of each pool
128   related to photosynthesis has been scaled to represent the fraction of leaf nitrogen associated with
129   it, in total accounting for 54% of leaf nitrogen. In the case of the photorespiratory cycle, this occurs
130   across three organelles. Within chloroplasts, about 16% of the nitrogen is associated with other
131   proteins and molecules not directly associated with photosynthesis and protein synthesis. For the

132 remainder of the cell, another 13% is left in the 'other' category that includes the nucleus, cytosol
133 and non-photorespiratory mitochondrial processes.

134

135 Scaling to the ecosystem

136   Given the diversity of plant species and ecosystems, it is a challenge to represent them
137 through generalisations. Leaf dry mass and nitrogen contents per unit area have been determined
138 for samples collected in the field for many species. For those leaves which also had photosynthetic
139 attributes measured in the field, relationships have emerged. Linear relationships between
140 photosynthetic capacity and leaf nitrogen content per unit area exist for different plant types (Kattge
141 *et al.*, 2009), although perhaps surprisingly, nitrogen fixing legumes overlap with non leguminous
142 dicotyledonous crop species (Adams *et al.*, 2018). Since there are many more measurements of leaf
143 nitrogen than photosynthesis on field grown material, these relationships between photosynthesis
144 and leaf nitrogen are widely embedded into ecosystem and global models. However, given the
145 variability in the slope relating photosynthetic capacity to leaf nitrogen content per unit area
146 between plant types, ground truthing is still required, e.g. arctic biomes (Rogers *et al.*, 2017b). Field
147 gas exchange can establish the relationship between Rubisco capacity and leaf nitrogen content,
148 although this may not reflect the actual allocation of nitrogen in Rubisco (Bahar *et al.*, 2017).
149 Improvements in remote sensing capability are increasing our ability to estimate plant
150 characteristics from reflectance spectra (Martin *et al.*, 2018). Whether it is possible to use
151 hyperspectral reflectance to derive estimates of Rubisco capacity directly (Serbin *et al.*, 2015; Silva-
152 Perez *et al.*, 2018; Yendrek *et al.*, 2017) or indirectly by first predicting nitrogen content (Dechant *et
153 al.*, 2017), is currently an active area of research.

154   Analysis of multiple publications revealed four features associated with increasing leaf mass
155 per unit area between species (Onoda *et al.*, 2017). Firstly, there was an apparent decrease in
156 nitrogen allocated to Rubisco. Secondly, there was a decrease in mesophyll conductance per unit of
157 mesophyll cell surface exposed to intercellular airspace. Thirdly, the draw-down in CO_2 partial
158 pressure between intercellular airspaces and the sites of carboxylation inside chloroplasts during
159 photosynthesis increased with increasing LMA. Fourthly, there was an increase in the fraction of leaf
160 nitrogen associated with the cell wall. The combination of these features reduces photosynthetic
161 capacity per unit of leaf N in species with greater LMA. Given that LMA is associated with leaf
162 lifespan, rather than achieving an instantaneous high photosynthetic rate per unit leaf nitrogen,
163 species with high LMA may instead achieve greater lifetime photosynthetic return from a given
164 investment of N into a leaf.

165

166 Fertilizer - photosynthesis - food

167   In the forty years 1962 - 2002, the combined global production of wheat, rice and maize
168 increased from 682 to 1752 Mt a^{-1} and nitrogen fertilizer production increased from 13.6 to 88.2 Mt
169 a^{-1} (http://www.fao.org/faostat/en/#data). There was a close linear relationship between these two,
170 with 13.8 tonnes of grain produced per tonne of nitrogen fertilizer. Assuming an average grain
171 nitrogen content for wheat, rice and maize of 1.9% (Jaksomsak *et al.*, 2017; Rapp *et al.*, 2018;
172 Uribelarrea *et al.*, 2008), harvested grain accounts for one quarter of global N fertilizer. This is
173 remarkable given that the fertilizer is not only applied to these three crops, that the harvested grain
174 represents only part of the nitrogen in the crop at maturity, that there are losses of nitrogen from
175 leaching, erosion and denitrification and there is some residual nitrogen left in the soil. However, the

176 environmental costs associated with nitrogen escape are a growing cause for concern and there are
177 pressing demands for improving the efficiency in the use of nitrogen applied in agriculture to reduce
178 environmental damage, economic cost and atmospheric greenhouse gas consequences both during
179 the production of fertilizer and NOx emissions from fields.

180 Plants need to balance carbon gain with the synthesis of organic nitrogen compounds. As a
181 consequence of the oxygenation reaction catalysed by Rubisco, the photorespiratory pathway
182 recycles 2 molecules of phosphoglycolate to produce one PGA. At the same time, one molecule of
183 ammonia is released in mitochondria and is refixed by GS GOGAT. The widely used Farquhar, von
184 Caemmerer and Berry biochemical model of C3 photosynthesis (Farquhar *et al.*, 1980) assumes
185 complete recycling, although this may not always be the case (Abadie *et al.*, 2017; Bloom and
186 Lancaster, 2018; Busch *et al.*, 2018). At 25 °C and current atmospheric CO_2 concentrations,
187 approximately 6 carbon atoms are fixed per ammonia recycled (see supplementary information). By
188 comparison, new biomass requires 33 carbon to be fixed for each new N, assuming the plant
189 contains 2% N, 40% C and respires 30% of daily carbon fixed during the production of this new
190 biomass. Incorporation of ammonia during photorespiration or de novo incorporation in leaves uses
191 the same GS GOGAT enzymatic pathway. Therefore, for plants converting inorganic N into organic
192 compounds in their leaves, 85% of the GS GOGAT flux is dealing with photorespiration on average.
193 At any instant, this proportion would change as it is affected by temperature, irradiance and CO_2
194 concentration. One consequence of rising atmospheric CO_2 concentrations is that the C:N balance of
195 plant tissue is changing. Elevated CO_2 reduces photorespiration and with the exception of legumes
196 that can fix atmospheric nitrogen symbiotically, plants grown under elevated atmospheric CO_2 have
197 lower nitrogen concentrations (Feng *et al.*, 2015). This translates into lower grain protein
198 concentrations which may have dietary implications in future (Myers *et al.*, 2014; Zhu *et al.*, 2018).

199

200 Engineering photosynthesis to improve crop yield

201 The detailed knowledge of photosynthesis has led to the identification of many proteins that
202 can be targeted to increase carbon gain. A selection of targets that have been identified are
203 presented in Box 4. In some cases, initial proof of concept has been obtained with transformed
204 model plants (Driever *et al.*, 2017; Kromdijk *et al.*, 2016; Lopez-Calcagno *et al.*, 2018; Salesse-Smith
205 *et al.*, 2018). Field trials with crop plants are underway and their outcome is eagerly awaited. Given
206 the central importance of Rubisco in determining the rates of CO_2 assimilation and photorespiration,
207 and because it accounts for so much of leaf nitrogen, much attention is focussed on ways to improve
208 its performance. Approaches fall into two categories. Firstly, those where the catalytic properties of
209 Rubisco are altered (e.g. from C4 species or other organisms, (Orr *et al.*, 2016)). Secondly, those
210 where the CO_2 partial pressure around Rubisco is increased (e.g. CO_2 concentrating mechanisms
211 such as carboxysomes (Hanson *et al.*, 2016; Long *et al.*, 2018; Rae *et al.*, 2017), greater mesophyll
212 conductance (Groszmann *et al.*, 2017) or photorespiratory bypass (Peterhansel and Maurino, 2011)).
213 While some variation in kinetic properties of Rubisco between wheat relatives has been identified
214 (Prins *et al.*, 2016), detailed crop modelling is needed to assess the impact and cost/benefit from
215 engineering an alternative form into elite wheat. While there are several crop models available
216 (Song *et al.*, 2017; Wu *et al.*, 2018; Yin and Struik, 2017), it is a complex task to deal with plant
217 functions that are not necessarily well represented or fully parameterised. The perennial debate
218 about whether plant growth and yield is determined by source photosynthesis or sink demand
219 continues. In the case of rice, increasing sink capacity led to a dramatic increase in yield (Ashikari *et*
220 *al.*, 2005). The current focus on improving photosynthesis is because the gains in harvest index (grain

221 yield / above ground biomass) associated with the introduction of dwarfing genes have been largely
222 maximised, but maintaining or increasing both sink strength and harvest index is also crucial.

223   If a plant could be engineered to fix more carbon per unit of nitrogen associated with
224 photosynthesis, then unless de novo incorporation of nitrogen was also enhanced, there would be a
225 lowering of the nitrogen concentration of the plant and most likely the protein content of the grain.
226 An increase in carbon gain per unit photosynthetic N could free up N for investment in new tissues
227 elsewhere and increase growth. This is observed when plants are grown under elevated
228 atmospheric CO_2 (Ainsworth and Long, 2005). However, unless additional organic N is incorporated
229 into other tissues, the conversion of that increased growth into greater yield would result in lower
230 grain protein. If the additional organic N incorporated elsewhere in the plant could not provide any
231 improvement above that gained from greater photosynthesis per unit of photosynthetic nitrogen,
232 what is the benefit from raising photosynthetic rate per unit N?

233   A second concern is that for cereal crops, nitrogen is remobilised from leaves and stems
234 during grain filling. At maturity, the grain can account for 80-90% of aboveground N (Barraclough *et
235 al.*, 2010; Gaju *et al.*, 2014). For a crop yielding 10 tonnes per hectare with a 2.5% N concentration in
236 the grain, this represents 250 kg N ha^{-1}. To contain this within a crop canopy with a leaf area index of
237 7 (Shearman *et al.*, 2005), the leaf nitrogen content would need to be 3.6 g m^{-2}. This is close to the
238 maximum leaf nitrogen content that is observed (Silva-Perez *et al.*, 2018). If increasing
239 photosynthesis per unit N resulted in lower N contents per unit leaf area, then a greater fraction of
240 this remobilisable N would need to be present in the sheath and stem fractions. In the case of
241 wheat, the ear can also make a substantial photosynthetic contribution to the grain (Maydup *et al.*,
242 2012; Zhou *et al.*, 2016). While these tissues can contribute to canopy photosynthesis, the relative
243 efficiency of leaf and stem needs to be investigated in order to assess the consequences. The point
244 is, that to increase yield while maintaining grain protein concentration requires increasing both
245 photosynthetic carbon gain and de novo N incorporation. In addition, the crop canopy has to be
246 capable of holding the vast majority of that N in its leaves to enable its relocation into developing
247 grain. An alternative is to continue de novo N incorporation during grain filling which requires
248 continued root growth, N uptake (perhaps associated with a late application of fertilizer) and
249 incorporation into protein while leaves are senescing.

250

251 Future

252   Given that Rubisco constitutes the largest fraction of nitrogen in leaves of C3 plants, it
253 justifiably attracts great attention. In the absence of complete kinetic information to describe the
254 performance of Rubisco from different species, the default has frequently been to assume kinetic
255 values of tobacco Rubisco (Bernacchi *et al.*, 2002). However, the kinetic properties of Rubisco from
256 diverse species need to be determined. Some of the variation between species in the apparent
257 Rubisco activity per unit leaf nitrogen might be associated with variation in kinetic properties, but
258 other factors could also be involved, such as different allocation of nitrogen towards Rubisco and
259 different activation state. With improved quantification of relative protein abundance, the extent to
260 which variation in nitrogen allocation to pigment protein complexes is associated with Rubisco
261 performance will be revealed. The limited number of species for which thylakoid N cost has been
262 quantified should be expanded. In particular, the N allocated to ATP synthase needs attention, given
263 its apparent significant cost.

264

265   Acknowledgements

270

271

272   Box 1. Key developments relating photosynthesis and nitrogen

273   • Leaf nitrogen budget: A tradeoff is apparent between nitrogen allocated to Rubisco versus
274   cell walls amongst plant functional types

275   In a meta analysis of C_3 species, Onoda et al. (2017) showed that with increasing leaf dry mass per
276   unit area, the fraction of leaf nitrogen allocated to Rubisco declined while that allocated to cell wall
277   material increased. Short lived leaves have greater photosynthetic rates per unit leaf nitrogen.

278   • Scaling to the ecosystem: Rubisco capacity per unit leaf nitrogen

279   Rubisco capacity (V_{cmax}) is commonly derived from gas exchange measurements, but this does not
280   always equate to Rubisco protein. For tropical rainforest trees (Bahar *et al.*, 2017) and Arctic tundra
281   (Rogers *et al.*, 2017b) new field data improves ecosystem models.

282   • Fertilizer, photosynthesis, food security: Rising atmospheric CO_2 reduces grain protein
283   concentration

284   Achieving and maintaining high cereal yields requires the use of nitrogen fertilizers, yet rising
285   atmospheric CO_2 is diminishing the grain quality (Zhu *et al.*, 2018). How can we diminish the negative
286   impact of fertilizer use while maintaining protein?

287   • Engineering photosynthesis: Protein targets that increase photosynthesis and biomass

288   Increasing a photosystem II protein and two enzymes that interconvert carotenoids to regulate
289   energy dissipation led to increased biomass production in field trials (Kromdijk *et al.*, 2016). There
290   are a growing number of candidate genes being investigated to enhance photosynthesis.

291

292

293   Box 2. The nitrogen cost of thylakoids in relation to their electron transport capacity.

294   Photosynthetic electron transport capacity is directly proportional to the cytochrome f content, 155
295   mol e⁻ (mol cyt f)$^{-1}$ s^{-1} (Evans, 1988; Niinemets and Tenhunen, 1997). A constant N cost associated
296   with pigment protein complexes of 37.3 mol N (mol Chl)$^{-1}$ is assumed (green rectangle). Thylakoid
297   nitrogen associated with photosynthetic electron transport (yellow triangle) is shown for two
298   different assumed costs (red lines). Data from (Evans, 1987; Evans and Seemann, 1989; Ghannoum
299   *et al.*, 2005; Terashima and Evans, 1988).
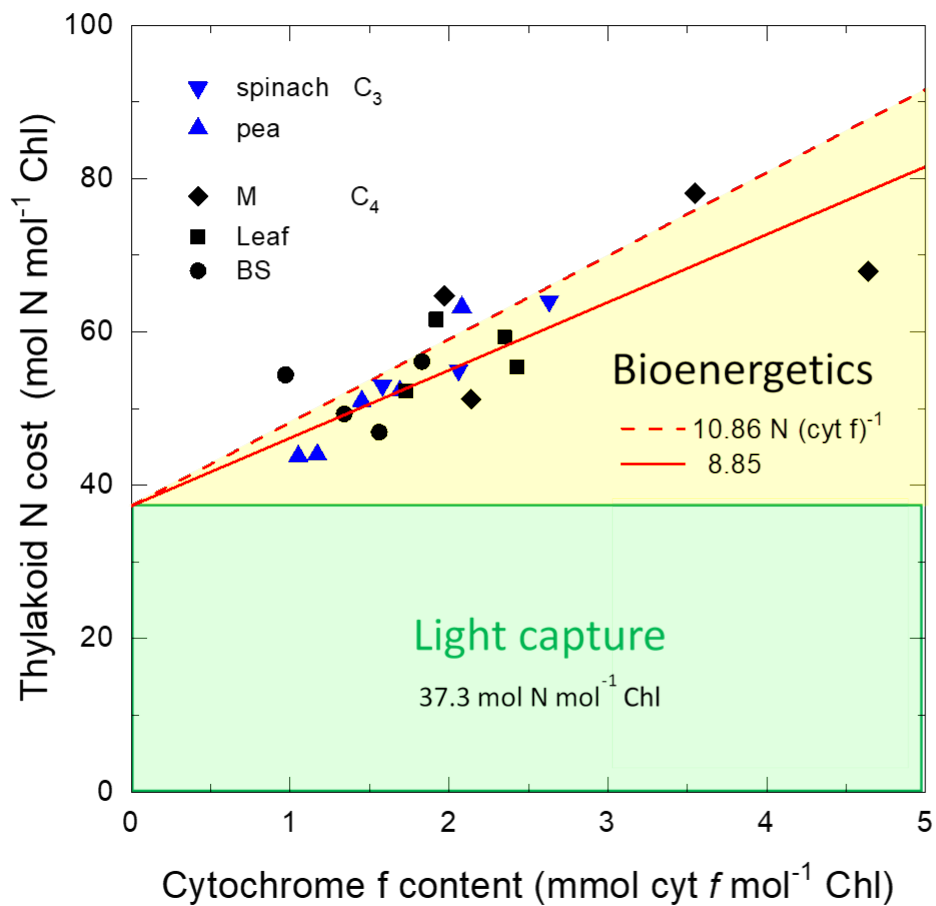
300

301

302 Box 3. Nitrogen budget for a C3 leaf cell.

303 The coloured shapes are scaled relative to their proportion of leaf N. The distribution of nitrogen
304 between different organelles is shown on the right hand side (see supplementary information). LHC
305 light harvesting chlorophyll a/b complex, PSII photosystem II reaction centre, PSI-LHCI photosystem I
306 reaction centre with its light harvesting chlorophyll a/b complex, ATPase ATP synthase, cyt f
307 cytochrome b_6f Rieske iron sulphur complex, RCA Rubisco activase, CA carbonic anhydrase, PCR
308 enzymes of the photosynthetic carbon reduction cycle excluding Rubisco, PCO enzymes in the
309 photosynthetic carbon oxidation cycle, Protein synth. N associated with protein synthesis including
310 amino acids.
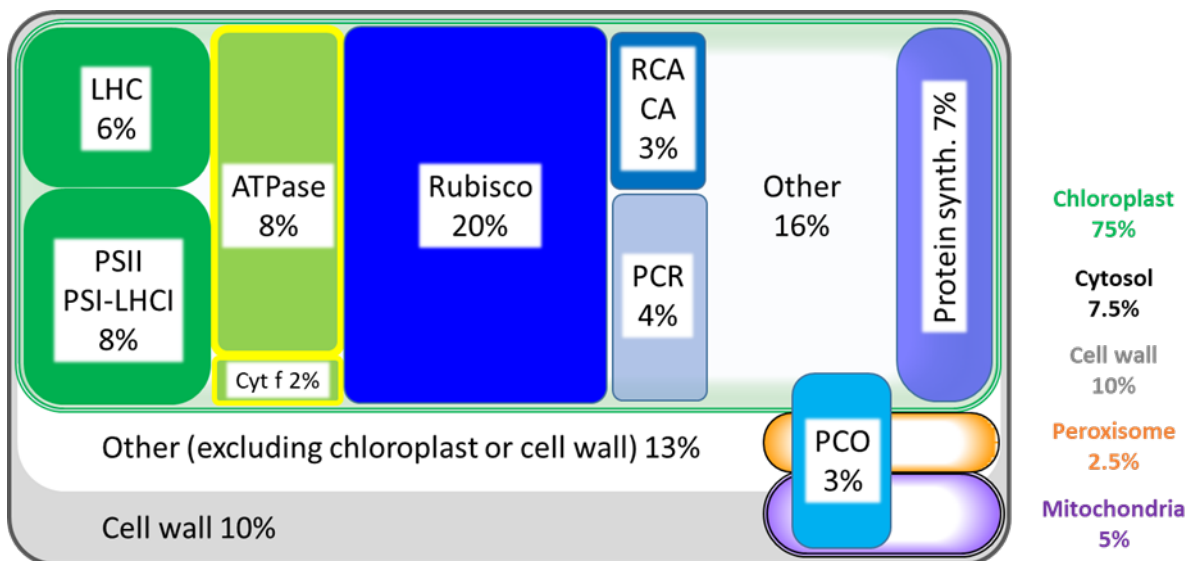
311

312

313

314   Box 4. Targets for improving photosynthesis

315   Many proteins have been identified which could potentially increase carbon gain and a selection is
316   shown. The numbering order reflects the nitrogen cost of adding additional proteins, beginning with
317   the greatest N requirement for Rubisco or ATP synthase. The protein cost associated with increased
318   expression of targets 3 to 6 is likely to be small. In the case of light harvesting complex, a reduction
319   in chlorophyll content per unit area frees up nitrogen that could be invested in other more rate
320   limiting photosynthetic proteins.

321

322

323   [refs – included for endnote referencing, not for printing
324   1 (Sharwood *et al.*, 2016a; Sharwood *et al.*, 2016b), 2 ATP synthase (Yamori *et al.*, 2011), 3
325   cytochrome b6f (Simkin *et al.*, 2017b), 4 PsbS VDE ZEP (Kromdijk *et al.*, 2016), 5 SBPase, FBP aldolase
326   (Driever *et al.*, 2017; Simkin *et al.*, 2017a), 6 Rubisco activase , 7 photorespiratory bypass (Ahmad *et
327   al.*, 2016; Dalal *et al.*, 2015; Kebeish *et al.*, 2007), 8 Glycine decarboxylase – H (Lopez-Calcagno *et al.*,
328   2018; Simkin *et al.*, 2017a), 9 light harvesting complex (Slattery *et al.*, 2017; Walker *et al.*, 2018)]

LIGHT

O_2

Triose-P

H_2O

RuBP

CO_2 **Rubisco** O_2

PGA

ATP NADPH

chloroplast

peroxisome

mitochondria

plant cell

CO_2 NH_3

1 **Rubisco** (Sharwood *et al.*, 2016a,b) Transferring superior Rubiscos into C_3 crops could increase photosynthesis.

2 **ATP synthase** (Yamori *et al.*, 2011) Antisense reduction of ATP synthase suggests that while this complex may not limit electron transport rate, an increased content would be needed to obtain the maximum benefit from increasing cyt b_6f content.

3 **Cytochrome b_6f** (Simkin *et al.*, 2017b) Overexpressing the Rieske FeS protein increased the content of cyt b6f complex, electron transport capacity and plant biomass in Arabidopsis.

4 **PsbS VDE ZEP** (Kromdijk *et al.*, 2016) Overexpression of these three proteins in tobacco increased the capacity for NPQ and the speed with which photoprotection cycles under dynamic light conditions in the field, leading to increased plant growth.

5 **SBPase, FBP aldolase** Two-fold overexpression of SBPase in wheat (Driever *et al.* 2017) and overexpression of SBPase / FBP aldolase in Arabidopsis (Simkin *et al.* 2017a) increased biomass.

High

N cost

Low

6 **Rubisco activase** Varying RCA by overexpression or antisense led to a decrease or increase, respectively, in Rubisco content in rice (Fukayama *et al.*, 2018).

7 **Photorespiratory bypass** Three enzymes in the glycolate catabolic pathway from *E. coli* bypass the normal photorespiratory cycle, releasing CO_2 within the chloroplast (Kebeish *et al.*, 2007). Both *Camelina* (Dalal *et al.* 2015) and potato (Ahmad *et al.* 2016) plants transformed with these genes produce more biomass.

8 **Glycine decarboxylase – H** Overexpression of GDC-H in Arabidopsis (Simkin *et al.*, 2017a) and tobacco (Lopez-Calcagno *et al.* 2018) led to an increase in biomass.

9 **Light harvesting complex** Soybean mutants with reduced chlorophyll contents demonstrate that reallocation of N away from chlorophyll protein complexes towards other photosynthetic proteins could increase crop canopy photosynthesis (Slattery *et al.*, 2017; Walker *et al.*, 2018).

329

13

330

Complex	MW (kDa)	# Chl	N/Chl mol N (mol Chl)$^{-1}$	% total Chl	N/Chl mol N (mol Chl)$^{-1}$
LHC	28.8	14	23.5	56	13.2
PSI - LHCI	388	156	28.4	30	8.5
PSII	456	63	82.7	14	11.6
Chl					4
Light harvesting					37.3

331

332 Table 1. Molecular weight, number of chlorophyll molecules per complex, protein nitrogen cost per
333 chlorophyll in the complex, percentage of the total chlorophyll associated with each complex and
334 nitrogen cost of each component weighted by abundance giving a total nitrogen cost associated with
335 light harvesting (updated from Evans and Seemann, 1989).

336

References

Abadie C, Lothier J, Boex-Fontvieille E, Carroll A, Tcherkez G. 2017. Direct assessment of the metabolic origin of carbon atoms in glutamate from illuminated leaves using 13C-NMR. *NEW PHYTOLOGIST* **216**, 1079-1089.

Adams MA, Buckley TN, Salter WT, Buchmann N, Blessing CH, Turnbull TL. 2018. Contrasting responses of crop legumes and cereals to nitrogen availability. *NEW PHYTOLOGIST* **217**, 1475-1483.

Ahmad R, Bilal M, Jeon JH, Kim HS, Park YI, Shah MM, Kwon SY. 2016. Improvement of biomass accumulation of potato plants by transformation of cyanobacterial photorespiratory glycolate catabolism pathway genes. *Plant Biotechnology Reports* **10**, 269-276.

Ainsworth EA, Long SP. 2005. What have we learned from 15 years of free-air CO_2 enrichment (FACE)? A meta-analytic review of the responses of photosynthesis, canopy. *NEW PHYTOLOGIST* **165**, 351-371.

Ashikari M, Sakakibara H, Lin SY, Yamamoto T, Takashi T, Nishimura A, Angeles ER, Qian Q, Kitano H, Matsuoka M. 2005. Cytokinin oxidase regulates rice grain production. *Science* **309**, 741-745.

Bahar NHA, Ishida FY, Weerasinghe LK, Guerrieri R, O'Sullivan OS, Bloomfield KJ, Asner GP, Martin RE, Lloyd J, Malhi Y, Phillips OL, Meir P, Salinas N, Cosio EG, Domingues TF, Quesada CA, Sinca F, Escudero Vega A, Zuloaga Ccorimanya PP, del Aguila-Pasquel J, Quispe Huaypar K, Cuba Torres I, Butrón Loayza R, Pelaez Tapia Y, Huaman Ovalle J, Long BM, Evans JR, Atkin OK. 2017. Leaf-level photosynthetic capacity in lowland Amazonian and high-elevation Andean tropical moist forests of Peru. *NEW PHYTOLOGIST* **214**, 1002-1018.

Barraclough PB, Howarth JR, Jones J, Lopez-Bellido R, Parmar S, Shepherd CE, Hawkesford MJ. 2010. Nitrogen efficiency of wheat: Genotypic and environmental variation and prospects for improvement. *European Journal of Agronomy* **33**, 1-11.

Bernacchi CJ, Portis AR, Nakano H, von Caemmerer S, Long SP. 2002. Temperature response of mesophyll conductance. Implications for the determination of Rubisco enzyme kinetics and for limitations to photosynthesis in vivo. *PLANT PHYSIOLOGY* **130**, 1992-1998.

Bloom AJ, Lancaster KM. 2018. Manganese binding to Rubisco could drive a photorespiratory pathway that increases the energy efficiency of photosynthesis. *Nature Plants* **10.1038/s41477-018-0191-0**.

Busch FA, Sage RF, Farquhar GD. 2018. Plants increase CO2 uptake by assimilating nitrogen via the photorespiratory pathway. *Nature Plants* **4**, 46-54.

Caspy I, Nelson N. 2018. Structure of the plant photosystem I. *Biochemical Society Transactions* **46**, 285-294.

Dalal J, Lopez H, Vasani NB, Hu ZH, Swift JE, Yalamanchili R, Dvora M, Lin XL, Xie DY, Qu RD, Sederoff HW. 2015. A photorespiratory bypass increases plant growth and seed yield in biofuel crop Camelina sativa. *Biotechnology for Biofuels* **8**.

Dechant B, Cuntz M, Vohland M, Schulz E, Doktor D. 2017. Estimation of photosynthesis traits from leaf reflectance spectra: Correlation to nitrogen content as the dominant mechanism. *Remote Sensing of Environment* **196**, 279-292.

Driever SM, Simkin AJ, Alotaibi S, Fisk SJ, Madgwick PJ, Sparks CA, Jones HD, Lawson T, Parry MAJ, Raines CA. 2017. Increased SBPase activity improves photosynthesis and grain yield in wheat grown in greenhouse conditions. *Philosophical Transactions of the Royal Society B: Biological Sciences* **372**.

Eckardt NA, Snyder GW, Portis Jr AR, Ogren WL. 1997. Growth and Photosynthesis under High and Low Irradiance of Arabidopsis thaliana Antisense Mutants with Reduced Ribulose-1,5-Bisphosphate Carboxylase/Oxygenase Activase Content. *PLANT PHYSIOLOGY* **113**, 575-586.

Evans JR. 1987. The relationship between electron transport components and photosynthetic capacity in pea leaves grown at different irradiances. *AUSTRALIAN JOURNAL OF PLANT PHYSIOLOGY* **14**, 157-170.

Evans JR. 1988. Acclimation by the thylakoid membranes to growth irradiance and the partitioning of nitrogen between soluble and thylakoid proteins. *AUSTRALIAN JOURNAL OF PLANT PHYSIOLOGY* **15**, 93-106.

388 **Evans JR, Seemann JR**. 1984. Differences between wheat genotypes in specific activity of ribulose-
389 1,5-bisphosphate carboxylase and the relationship to photosynthesis. *PLANT PHYSIOLOGY* **74**, 759-
390 765.
391 **Evans JR, Seemann JR**. 1989. The allocation of protein nitrogen in the photosynthetic apparatus:
392 costs, consequences, and control. In: Briggs WR, ed. *Photosynthesis*: A.R. Liss, New York, 183-205.
393 **Farquhar GD, von Caemmerer S, Berry JA**. 1980. A biochemical model of photosynthetic CO_2
394 assimilation in leaves of C_3 species. *PLANTA* **149**, 78-90.
395 **Feng ZZ, Rutting T, Pleijel H, Wallin G, Reich PB, Kammann CI, Newton PCD, Kobayashi K, Luo YJ,**
396 **Uddling J**. 2015. Constraints to nitrogen acquisition of terrestrial plants under elevated CO2. *GLOBAL*
397 *CHANGE BIOLOGY* **21**, 3152-3168.
398 **Gaju O, Allard V, Martre P, Le Gouis J, Moreau D, Bogard M, Hubbart S, Foulkes MJ**. 2014. Nitrogen
399 partitioning and remobilization in relation to leaf senescence, grain yield and grain nitrogen
400 concentration in wheat cultivars. *Field Crops Research* **155**, 213-223.
401 **Ghannoum O, Evans JR, Chow WS, Andrews TJ, Conroy JP, von Caemmerer S**. 2005. Faster rubisco
402 is the key to superior nitrogen-use efficiency in NADP-malic enzyme relative to NAD-malic enzyme C-
403 4 grasses. *PLANT PHYSIOLOGY* **137**, 638-650.
404 **Groszmann M, Osborn HL, Evans JR**. 2017. Carbon dioxide and water transport through plant
405 aquaporins. *Plant, Cell & Environment* **40**, 938-961.
406 **Hanson MR, Lin MT, Carmo-Silva AE, Parry MAJ**. 2016. Towards engineering carboxysomes into C3
407 plants. *Plant Journal* **87**, 38-50.
408 **Jaksomsak P, Rerkasem B, Prom-u-thai C**. 2017. Responses of grain zinc and nitrogen concentration
409 to nitrogen fertilizer application in rice varieties with high-yielding low-grain zinc and low-yielding
410 high grain zinc concentration. *PLANT AND SOIL* **411**, 101-109.
411 **Kattge J, DÍAz S, Lavorel S, Prentice IC, Leadley P, BÖNisch G, Garnier E, Westoby M, Reich PB,**
412 **Wright IJ, Cornelissen JHC, Violle C, Harrison SP, Van Bodegom PM, Reichstein M, Enquist BJ,**
413 **Soudzilovskaia NA, Ackerly DD, Anand M, Atkin O, Bahn M, Baker TR, Baldocchi D, Bekker R,**
414 **Blanco CC, Blonder B, Bond WJ, Bradstock R, Bunker DE, Casanoves F, Cavender-Bares J, Chambers**
415 **JQ, Chapin Iii FS, Chave J, Coomes D, Cornwell WK, Craine JM, Dobrin BH, Duarte L, Durka W, Elser**
416 **J, Esser G, Estiarte M, Fagan WF, Fang J, FernÁNdez-MÉNdez F, Fidelis A, Finegan B, Flores O, Ford**
417 **H, Frank D, Freschet GT, Fyllas NM, Gallagher RV, Green WA, Gutierrez AG, Hickler T, Higgins SI,**
418 **Hodgson JG, Jalili A, Jansen S, Joly CA, Kerkhoff AJ, Kirkup D, Kitajima K, Kleyer M, Klotz S, Knops**
419 **JMH, Kramer K, KÜHn I, Kurokawa H, Laughlin D, Lee TD, Leishman M, Lens F, Lenz T, Lewis SL,**
420 **Lloyd J, LlusiÀ J, Louault F, Ma S, Mahecha MD, Manning P, Massad T, Medlyn BE, Messier J, Moles**
421 **AT, MÜLler SC, Nadrowski K, Naeem S, Niinemets Ü, NÖLlert S, NÜSke A, Ogaya R, Oleksyn J,**
422 **Onipchenko VG, Onoda Y, OrdoÑEz J, Overbeck G, Ozinga WA, PatiÑO S, Paula S, Pausas JG,**
423 **PeÑUelas J, Phillips OL, Pillar V, Poorter H, Poorter L, Poschlod P, Prinzing A, Proulx R, Rammig A,**
424 **Reinsch S, Reu B, Sack L, Salgado-Negret B, Sardans J, Shiodera S, Shipley B, Siefert A, Sosinski E,**
425 **Soussana JF, Swaine E, Swenson N, Thompson K, Thornton P, Waldram M, Weiher E, White M,**
426 **White S, Wright SJ, Yguel B, Zaehle S, Zanne AE, Wirth C**. 2011. TRY – a global database of plant
427 traits. *GLOBAL CHANGE BIOLOGY* **17**, 2905-2935.
428 **Kattge J, Knorr W, Raddatz T, Wirth C**. 2009. Quantifying photosynthetic capacity and its
429 relationship to leaf nitrogen content for global-scale terrestrial biosphere models. *GLOBAL CHANGE*
430 *BIOLOGY* **15**, 976-991.
431 **Kebeish R, Niessen M, Thiruveedhi K, Bari R, Hirsch HJ, Rosenkranz R, Stabler N, Schonfeld B,**
432 **Kreuzaler F, Peterhansel C**. 2007. Chloroplastic photorespiratory bypass increases photosynthesis
433 and biomass production in *Arabidopsis thaliana*. *Nature Biotechnology* **25**, 593-599.
434 **Kromdijk J, Głowacka K, Leonelli L, Gabilly ST, Iwai M, Niyogi KK, Long SP**. 2016. Improving
435 photosynthesis and crop productivity by accelerating recovery from photoprotection. *Science* **354**,
436 857-861.
437 **Law KP, Lim YP**. 2013. Recent advances in mass spectrometry: data independent analysis and hyper
438 reaction monitoring. *Expert Review of Proteomics* **10**, 551-566.

439 **Leong T-Y, Anderson JM**. 1984. Adaptation of the thylakoid membranes of pea chloroplasts to light
440 intensities. I. Study on the distribution of chlorophyll-protein complexes. *PHOTOSYNTHESIS*
441 *RESEARCH* **5**, 105-115.
442 **Li L, Nelson CJ, Trosch J, Castleden I, Huang SB, Millar AH**. 2017. Protein Degradation Rate in
443 Arabidopsis thaliana Leaf Growth and Development. *Plant Cell* **29**, 207-228.
444 **Liu ZF, Yan HC, Wang KB, Kuang TY, Zhang JP, Gui LL, An XM, Chang WR**. 2004. Crystal structure of
445 spinach major light-harvesting complex at 2.72 angstrom resolution. *Nature* **428**, 287-292.
446 **Long BM, Hee WY, Sharwood RE, Rae BD, Kaines S, Lim YL, Nguyen ND, Massey B, Bala S, von**
447 **Caemmerer S, Badger MR, Price GD**. 2018. Carboxysome encapsulation of the CO2-fixing enzyme
448 Rubisco in tobacco chloroplasts. *Nature Communications* **9**.
449 **Lopez-Calcagno PE, Fisk S, Brown KL, Bull SE, South PF, Raines CA**. 2018. Overexpressing the H-
450 protein of the glycine cleavage system increases biomass yield in glasshouse and field grown
451 transgenic tobacco plants. *Plant Biotechnology Journal*.
452 **Lundgren DH, Hwang SI, Wu LF, Han DK**. 2010. Role of spectral counting in quantitative proteomics.
453 *Expert Review of Proteomics* **7**, 39-53.
454 **Makino A, Osmond B**. 1991. Effects of nitrogen nutrition on nitrogen partitioning between
455 chloroplasts and mitochondria in pea and wheat. *PLANT PHYSIOLOGY* **96**, 355-362.
456 **Martin RE, Chadwick KD, Brodrick PG, Carranza-Jimenez L, Vaughn NR, Asner GP**. 2018. An
457 Approach for Foliar Trait Retrieval from Airborne Imaging Spectroscopy of Tropical Forests. *Remote*
458 *Sensing* **10**.
459 **Maydup ML, Antonietta M, Guiamet JJ, Tambussi EA**. 2012. The contribution of green parts of the
460 ear to grain filling in old and modern cultivars of bread wheat (Triticum aestivum L.): Evidence for
461 genetic gains over the past century. *Field Crops Research* **134**, 208-215.
462 **Myers SS, Zanobetti A, Kloog I, Huybers P, Leakey ADB, Bloom AJ, Carlisle E, Dietterich LH,**
463 **Fitzgerald G, Hasegawa T, Holbrook NM, Nelson RL, Ottman MJ, Raboy V, Sakai H, Sartor KA,**
464 **Schwartz J, Seneweera S, Tausz M, Usui Y**. 2014. Increasing CO2 threatens human nutrition. *Nature*
465 **510**, 139-+.
466 **Niinemets U, Tenhunen JD**. 1997. A model separating leaf structural and physiological effects on
467 carbon gain along light gradients for the shade-tolerant species *Acer saccharum. Plant, Cell and*
468 *Environment* **20**, 845-866.
469 **Onoda Y, Wright IJ, Evans JR, Hikosaka K, Kitajima K, Niinemets U, Poorter H, Tosens T, Westoby**
470 **M**. 2017. Physiological and structural tradeoffs underlying the leaf economics spectrum. *NEW*
471 *PHYTOLOGIST* **214**, 1447-1463.
472 **Orr DJ, Alcântara A, Kapralov MV, Andralojc PJ, Carmo-Silva E, Parry MAJ**. 2016. Surveying Rubisco
473 Diversity and Temperature Response to Improve Crop Photosynthetic Efficiency. *PLANT PHYSIOLOGY*
474 **172**, 707-717.
475 **Peterhansel C, Maurino VG**. 2011. Photorespiration redesigned. *PLANT PHYSIOLOGY* **155**, 49-55.
476 **Prins A, Orr DJ, Andralojc PJ, Reynolds MP, Carmo-Silva E, Parry MAJ**. 2016. Rubisco catalytic
477 properties of wild and domesticated relatives provide scope for improving wheat photosynthesis.
478 *JOURNAL OF EXPERIMENTAL BOTANY* **67**, 1827-1838.
479 **Rae BD, Long BM, Forster B, Nguyen ND, Velanis CN, Atkinson N, Hee WY, Mukherjee B, Price GD,**
480 **McCormick AJ**. 2017. Progress and challenges of engineering a biophysical CO2-concentrating
481 mechanism into higher plants. *JOURNAL OF EXPERIMENTAL BOTANY* **68**, 3717-3737.
482 **Rapp M, Lein V, Lacoudre F, Lafferty J, Müller E, Vida G, Bozhanova V, Ibraliu A, Thorwarth P,**
483 **Piepho HP, Leiser WL, Würschum T, Longin CFH**. 2018. Simultaneous improvement of grain yield
484 and protein content in durum wheat by different phenotypic indices and genomic selection.
485 *Theoretical and applied genetics* **131**, 1315-1329.
486 **Rogers A, Medlyn BE, Dukes JS, Bonan G, von Caemmerer S, Dietze MC, Kattge J, Leakey ADB,**
487 **Mercado LM, Niinemets U, Prentice IC, Serbin SP, Sitch S, Way DA, Zaehle S**. 2017a. A roadmap for
488 improving the representation of photosynthesis in Earth system models. *NEW PHYTOLOGIST* **213**,
489 22-42.

490 **Rogers A, Serbin SP, Ely KS, Sloan VL, Wullschleger SD**. 2017b. Terrestrial biosphere models
491 underestimate photosynthetic capacity and CO2 assimilation in the Arctic. *NEW PHYTOLOGIST* **216**,
492 1090-1103.
493 **Salesse-Smith CE, Sharwood RE, Busch FA, Kromdijk J, Bardal V, Stern DB**. 2018. Overexpression of
494 Rubisco subunits with RAF1 increases Rubisco content in maize. *Nature Plants* **4**, 802-810.
495 **Scheller HV, Jensen PE, Haldrup A, Lunde C, Knoetzel J**. 2001. Role of subunits in eukaryotic
496 Photosystem I. *Biochimica Et Biophysica Acta-Bioenergetics* **1507**, 41-60.
497 **Serbin SP, Singh A, Desai AR, Dubois SG, Jablonsld AD, Kingdon CC, Kruger EL, Townsend PA**. 2015.
498 Remotely estimating photosynthetic capacity, and its response to temperature, in vegetation
499 canopies using imaging spectroscopy. *Remote Sensing of Environment* **167**, 78-87.
500 **Sharwood RE, Ghannoum O, Kapralov MV, Gunn LH, Whitney SM**. 2016a. Temperature responses
501 of Rubisco from Paniceae grasses provide opportunities for improving C3 photosynthesis. *Nature*
502 *Plants* **2**, 16186.
503 **Sharwood RE, Ghannoum O, Whitney SM**. 2016b. Prospects for improving CO2 fixation in C3-crops
504 through understanding C4-Rubisco biogenesis and catalytic diversity. *Current Opinion in Plant*
505 *Biology* **31**, 135-142.
506 **Shearman VJ, Sylvester-Bradley R, Scott RK, Foulkes MJ**. 2005. Physiological processes associated
507 with wheat yield progress in the UK. *Crop Science* **45**, 175-185.
508 **Silva-Perez V, Molero G, Serbin SP, Condon AG, Reynolds MP, Furbank RT, Evans JR**. 2018.
509 Hyperspectral reflectance as a tool to measure biochemical and physiological traits in wheat.
510 *JOURNAL OF EXPERIMENTAL BOTANY* **69**, 483-496.
511 **Simkin AJ, Lopez-Calcagno PE, Davey PA, Headland LR, Lawson T, Timm S, Bauwe H, Raines CA**.
512 2017a. Simultaneous stimulation of sedoheptulose 1,7-bisphosphatase, fructose 1,6-bisphophate
513 aldolase and the photorespiratory glycine decarboxylase-H protein increases CO2 assimilation,
514 vegetative biomass and seed yield in Arabidopsis. *Plant Biotechnology Journal* **15**, 805-816.
515 **Simkin AJ, McAusland L, Lawson T, Raines CA**. 2017b. Overexpression of the RieskeFeS Protein
516 Increases Electron Transport Rates and Biomass Yield. *PLANT PHYSIOLOGY* **175**, 134-145.
517 **Slattery RA, VanLoocke A, Bernacchi CJ, Zhu XG, Ort DR**. 2017. Photosynthesis, Light Use Efficiency,
518 and Yield of Reduced-Chlorophyll Soybean Mutants in Field Conditions. *Frontiers in Plant Science* **8**.
519 **Song Q, Chen D, Long SP, Zhu X-G**. 2017. A user-friendly means to scale from the biochemistry of
520 photosynthesis to whole crop canopies and production in time and space – development of Java
521 WIMOVAC. *Plant, Cell & Environment* **40**, 51-55.
522 **Suzuki Y, Makino A, Mae T**. 2001. An efficient method for extraction of RNA from rice leaves at
523 different ages using benzyl chloride. *JOURNAL OF EXPERIMENTAL BOTANY* **52**, 1575-1579.
524 **Terashima I, Evans JR**. 1988. Effects of light and nitrogen nutrition on the organization of the
525 photosynthetic apparatus in spinach. *PLANT AND CELL PHYSIOLOGY* **29**, 143-155.
526 **Uribelarrea M, Crafts-Brandner SJ, Below FE**. 2008. Physiological N response of field-grown maize
527 hybrids (Zea mays L.) with divergent yield potential and grain protein concentration. *PLANT AND*
528 *SOIL* **316**, 151.
529 **von Caemmerer S**. 2000. *Biochemical models of leaf photosynthesis*. Collingwood, Victoria
530 (Australia): CSIRO publishing.
531 **Walker BJ, Drewry DT, Slattery RA, VanLoocke A, Cho YB, Ort DR**. 2018. Chlorophyll Can Be
532 Reduced in Crop Canopies with Little Penalty to Photosynthesis. *PLANT PHYSIOLOGY* **176**, 1215.
533 **Wang MC, Herrmann CJ, Simonovic M, Szklarczyk D, von Mering C**. 2015. Version 4.0 of PaxDb:
534 Protein abundance data, integrated across model organisms, tissues, and cell-lines. *Proteomics* **15**,
535 3163-3168.
536 **Wei X, Su X, Cao P, Liu X, Chang W, Li M, Zhang X, Liu Z**. 2016. Structure of spinach photosystem II-
537 LHCII supercomplex at 3.2 angstrom resolution. *Nature* **534**, 69-+.
538 **Wu A, Doherty A, Farquhar GD, Hammer GL**. 2018. Simulating daily field crop canopy
539 photosynthesis: an integrated software package. *FUNCTIONAL PLANT BIOLOGY* **45**, 362-377.

540 **Yamori W, Takahashi S, Makino A, Price GD, Badger MR, von Caemmerer S**. 2011. The roles of ATP
541 synthase and the cytochrome b_6/f complexes in limiting chloroplast electron transport and
542 determining photosynthetic capacity. *PLANT PHYSIOLOGY* **155**, 956-962.
543 **Yendrek CR, Tomaz T, Montes CM, Cao Y, Morse AM, Brown PJ, McIntyre LM, Leakey ADB,**
544 **Ainsworth EA**. 2017. High-Throughput Phenotyping of Maize Leaf Physiological and Biochemical
545 Traits Using Hyperspectral Reflectance. *PLANT PHYSIOLOGY* **173**, 614-626.
546 **Yin XY, Struik PC**. 2017. Can increased leaf photosynthesis be converted into higher crop mass
547 production? A simulation study for rice using the crop model GECROS. *JOURNAL OF EXPERIMENTAL*
548 *BOTANY* **68**, 2345-2360.
549 **Zhou BW, Serret MD, Elazab A, Bort Pie J, Araus JL, Aranjuelo I, Sanz-Saez A**. 2016. Wheat ear
550 carbon assimilation and nitrogen remobilization contribute significantly to grain yield. *Journal of*
551 *Integrative Plant Biology* **58**, 914-926.
552 **Zhu C, Kobayashi K, Loladze I, Zhu J, Jiang Q, Xu X, Liu G, Seneweera S, Ebi KL, Drewnowski A,**
553 **Fukagawa NK, Ziska LH**. 2018. Carbon dioxide (CO_2) levels this century will alter the protein,
554 micronutrients, and vitamin content of rice grains with potential health consequences for the
555 poorest rice-dependent countries. *Science Advances* **4**.

556

557

558 Supplementary information

559   1. Rescaling PaxDb to account for Rubisco abundance

560 The fraction of leaf nitrogen accounted for by Rubisco varies between C3 species, ranging from 10 to 30% and decreasing with increasing leaf dry mass per
561 unit leaf area e.g. (Onoda *et al.*, 2017). For Arabidopsis, Rubisco represents 40% of soluble protein (Eckardt *et al.*, 1997). In wheat, Rubisco represents about
562 20% of leaf nitrogen (Evans and Seemann, 1984). Assuming 7% of leaf nitrogen is not associated with protein (RNA and DNA, 3.6% of leaf nitrogen (rice,
563 (Suzuki *et al.*, 2001)), chlorophyll 1.6- 2.4% of leaf nitrogen, 1-2% other (e.g. other lipids, amino acids, alkaloids), then Rubisco represents 20/0.93 = 21.5%
564 of total protein. In the PaxDb, the abundance (ppm) is multiplied by the MW of each protein and summed to estimate total protein. By increasing the
565 abundance of both the large and small subunits of Rubisco in PaxDb to 119,000, Rubisco represented 21.5% of total protein, or 20% of leaf nitrogen.

566   2. Nitrogen cost of bioenergetics.

567 Three protein complexes are combined: cytochrome b_6f complex, ATP synthase and Fd NADP reductase. The relative abundance of the protein subunits is
568 taken from the PaxDb (Wang *et al.*, 2015) and normalised to PETC. For ATP synthase, the abundance is calculated by averaging four of the protein subunits,
569 assuming each ATP synthase contains 3 alpha, 3 beta, 1 delta and 1 epsilon subunits. For FNR, there are two subunits and the average relative abundance is
570 assumed.

Complex			PaxDb (ppm)	complex (ppm)	Complex ratio to PETC	MW (kDa)	N cost (mol N (mol cyt f)$^{-1}$)
cyt b6f	AT4G03280	PETC	3921	3921	1	101	1.15
ATP synthase	ATCG00120	3 ATPase alpha	15621	5207			
	ATCG00480	3 ATPase beta	16540	5513			
	AT4G09650	1 ATPase delta	5238	5238			
	ATCG00470	1 ATPase epsilon	5277	5277			
avg				**5309**	1.35	575	8.90
Fd NADP reductase	AT5G66190	FNR1	3244				
	AT1G20020	FNR2	3507				
avg				**3376**	0.86	82	0.81
Total							10.86

571

572

573   3.   Nitrogen distribution within the cell

574   75%   chloroplast (75-80%, pea, (Makino and Osmond, 1991); PaxDb (Wang et al. 2015 with gene annotation by (Li *et al.*, 2017), Arabidopsis
575   plastid 77% of total protein)

576   10%   cell wall (Onoda et al., 2017)

577   5%   mitochondria (5-10%, pea, Makino & Osmond, 1991; PaxDb (Wang et al. 2015 with gene annotation by Li et al. 2017) Arabidopsis
578   mitochondria 3.7% of total protein)

579   2.5%   peroxisome (PaxDb (Wang et al. 2015 with gene annotation by Li et al. 2017) Arabidopsis)

580   7.5%   other (cytosol, nucleus)

581

582   4.   Nitrogen fixed per carbon assimilated

583   The ratio of Rubisco carboxylations to ammonia recycled during photorespiration is derived from $2V_c/V_o = C/\Gamma^*$ (von Caemmerer, 2000) Eq 2.16, 2.18,
584   where the CO_2 partial pressure in the chloroplast, C, is assumed to be 60% of ambient (400 x 0.6 μbar) and the CO_2 compensation point in the absence
585   of mitochondrial CO_2 release, $\Gamma^* = 40$ μbar. One ammonia is recycled per two oxygenations, occurring every 6 carboxylations. By contrast, if new plant
586   biomass contains 40% C and 2% N, i.e. C;N ratio of 23.3, and 30% of daily fixed carbon is respired during the construction of new biomass, 23.3/0.7 =
587   33.3 C need to be fixed per N gained in new biomass. These 33.3 C were associated with the recycling of 33.3/6 = 5.6 ammonia. For plants converting
588   ammonia to organic compounds only in their leaves, the photorespiratory flux of ammonia thus represents 5.6/(5.6 + 1) = 0.85, or 85% of the GS
589   GOGAT flux.

590

591 References

592 **Eckardt NA, Snyder GW, Portis Jr AR, Ogren WL**. 1997. Growth and Photosynthesis under High and Low Irradiance of Arabidopsis thaliana Antisense
593 Mutants with Reduced Ribulose-1,5-Bisphosphate Carboxylase/Oxygenase Activase Content. *PLANT PHYSIOLOGY* **113**, 575-586.
594 **Evans JR, Seemann JR**. 1984. Differences between wheat genotypes in specific activity of ribulose-1,5-bisphosphate carboxylase and the relationship to
595 photosynthesis. *PLANT PHYSIOLOGY* **74**, 759-765.

596   **Li L, Nelson CJ, Trosch J, Castleden I, Huang SB, Millar AH**. 2017. Protein Degradation Rate in Arabidopsis thaliana Leaf Growth and Development. *Plant Cell*
597   **29**, 207-228.
598   **Makino A, Osmond B**. 1991. Effects of nitrogen nutrition on nitrogen partitioning between chloroplasts and mitochondria in pea and wheat. *PLANT*
599   *PHYSIOLOGY* **96**, 355-362.
600   **Onoda Y, Wright IJ, Evans JR, Hikosaka K, Kitajima K, Niinemets U, Poorter H, Tosens T, Westoby M**. 2017. Physiological and structural tradeoffs
601   underlying the leaf economics spectrum. *NEW PHYTOLOGIST* **214**, 1447-1463.
602   **Suzuki Y, Makino A, Mae T**. 2001. An efficient method for extraction of RNA from rice leaves at different ages using benzyl chloride. *JOURNAL OF*
603   *EXPERIMENTAL BOTANY* **52**, 1575-1579.
604   **von Caemmerer S**. 2000. *Biochemical models of leaf photosynthesis*. Collingwood, Victoria (Australia): CSIRO publishing.
605   **Wang MC, Herrmann CJ, Simonovic M, Szklarczyk D, von Mering C**. 2015. Version 4.0 of PaxDb: Protein abundance data, integrated across model
606   organisms, tissues, and cell-lines. *Proteomics* **15**, 3163-3168.

607

608

609 Supplementary information

610   5. Rescaling PaxDb to account for Rubisco abundance

611 The fraction of leaf nitrogen accounted for by Rubisco varies between C3 species, ranging from 10 to 30% and decreasing with increasing leaf dry mass per
612 unit leaf area e.g. (Onoda *et al.*, 2017). For Arabidopsis, Rubisco represents 40% of soluble protein (Eckardt *et al.*, 1997). In wheat, Rubisco represents about
613 20% of leaf nitrogen (Evans and Seemann, 1984). Assuming 7% of leaf nitrogen is not associated with protein (RNA and DNA, 3.6% of leaf nitrogen (rice,
614 (Suzuki *et al.*, 2001)), chlorophyll 1.6- 2.4% of leaf nitrogen, 1-2% other (e.g. other lipids, amino acids, alkaloids), then Rubisco represents 20/0.93 = 21.5%
615 of total protein. In the PaxDb, the abundance (ppm) is multiplied by the MW of each protein and summed to estimate total protein. By increasing the
616 abundance of both the large and small subunits of Rubisco in PaxDb to 119,000, Rubisco represented 21.5% of total protein, or 20% of leaf nitrogen.

617   6. Nitrogen cost of bioenergetics.

618 Three protein complexes are combined: cytochrome b_6f complex, ATP synthase and Fd NADP reductase. The relative abundance of the protein subunits is
619 taken from the PaxDb (Wang *et al.*, 2015) and normalised to PETC. For ATP synthase, the abundance is calculated by averaging four of the protein subunits,
620 assuming each ATP synthase contains 3 alpha, 3 beta, 1 delta and 1 epsilon subunits. For FNR, there are two subunits and the average relative abundance is
621 assumed.

Complex			PaxDb (ppm)	complex (ppm)	Complex ratio to PETC	MW (kDa)	N cost (mol N (mol cyt f)$^{-1}$)
cyt b6f	AT4G03280	PETC	3921	3921	1	101	1.15
ATP synthase	ATCG00120	3 ATPase alpha	15621	5207			
	ATCG00480	3 ATPase beta	16540	5513			
	AT4G09650	1 ATPase delta	5238	5238			
	ATCG00470	1 ATPase epsilon	5277	5277			
avg				**5309**	1.35	575	8.90
Fd NADP reductase	AT5G66190	FNR1	3244				
	AT1G20020	FNR2	3507				
avg				**3376**	0.86	82	0.81
Total							10.86

622

623   7. Nitrogen distribution within the cell

624   75%   chloroplast (75-80%, pea, (Makino and Osmond, 1991); PaxDb (Wang et al. 2015 with gene annotation by (Li *et al.*, 2017), Arabidopsis
625   plastid 77% of total protein)

626   10%   cell wall (Onoda et al., 2017)

627   5%   mitochondria (5-10%, pea, Makino & Osmond, 1991; PaxDb (Wang et al. 2015 with gene annotation by Li et al. 2017) Arabidopsis
628   mitochondria 3.7% of total protein)

629   2.5%   peroxisome (PaxDb (Wang et al. 2015 with gene annotation by Li et al. 2017) Arabidopsis)

630   7.5%   other (cytosol, nucleus)

631

632   8. Nitrogen fixed per carbon assimilated

633   The ratio of Rubisco carboxylations to ammonia recycled during photorespiration is derived from $2V_c/V_o = C/\Gamma^*$ (von Caemmerer, 2000) Eq 2.16, 2.18,
634   where the CO_2 partial pressure in the chloroplast, C, is assumed to be 60% of ambient (400 x 0.6 µbar) and the CO_2 compensation point in the absence
635   of mitochondrial CO_2 release, $\Gamma^* = 40$ µbar. One ammonia is recycled per two oxygenations, occurring every 6 carboxylations. By contrast, if new plant
636   biomass contains 40% C and 2% N, i.e. C;N ratio of 23.3, and 30% of daily fixed carbon is respired during the construction of new biomass, 23.3/0.7 =
637   33.3 C need to be fixed per N gained in new biomass. These 33.3 C were associated with the recycling of 33.3/6 = 5.6 ammonia. For plants converting
638   ammonia to organic compounds only in their leaves, the photorespiratory flux of ammonia thus represents 5.6/(5.6 + 1) = 0.85, or 85% of the GS
639   GOGAT flux.

640

641   References

642   **Eckardt NA, Snyder GW, Portis Jr AR, Ogren WL**. 1997. Growth and Photosynthesis under High and Low Irradiance of Arabidopsis thaliana Antisense
643   Mutants with Reduced Ribulose-1,5-Bisphosphate Carboxylase/Oxygenase Activase Content. *PLANT PHYSIOLOGY* **113**, 575-586.
644   **Evans JR, Seemann JR**. 1984. Differences between wheat genotypes in specific activity of ribulose-1,5-bisphosphate carboxylase and the relationship to
645   photosynthesis. *PLANT PHYSIOLOGY* **74**, 759-765.
646   **Li L, Nelson CJ, Trosch J, Castleden I, Huang SB, Millar AH**. 2017. Protein Degradation Rate in Arabidopsis thaliana Leaf Growth and Development. *Plant Cell*
647   **29**, 207-228.

648   **Makino A, Osmond B**. 1991. Effects of nitrogen nutrition on nitrogen partitioning between chloroplasts and mitochondria in pea and wheat. *PLANT*
649   *PHYSIOLOGY* **96**, 355-362.
650   **Onoda Y, Wright IJ, Evans JR, Hikosaka K, Kitajima K, Niinemets U, Poorter H, Tosens T, Westoby M**. 2017. Physiological and structural tradeoffs
651   underlying the leaf economics spectrum. *NEW PHYTOLOGIST* **214**, 1447-1463.
652   **Suzuki Y, Makino A, Mae T**. 2001. An efficient method for extraction of RNA from rice leaves at different ages using benzyl chloride. *JOURNAL OF*
653   *EXPERIMENTAL BOTANY* **52**, 1575-1579.
654   **von Caemmerer S**. 2000. *Biochemical models of leaf photosynthesis*. Collingwood, Victoria (Australia): CSIRO publishing.
655   **Wang MC, Herrmann CJ, Simonovic M, Szklarczyk D, von Mering C**. 2015. Version 4.0 of PaxDb: Protein abundance data, integrated across model
656   organisms, tissues, and cell-lines. *Proteomics* **15**, 3163-3168.

657

658